Bulletin of Mathematical Biology (2007)
DOI 10.1007/s11538-007-9195-z

ORIGINAL ARTICLE

Mathematical Model of BCG Immunotherapy in Superficial Bladder Cancer

Svetlana Bunimovich-Mendrazitsky[a], Eliezer Shochat[b], Lewi Stone[a,*]

[a] *Biomathematics Unit, Department of Zoology, Faculty of Life Science, Tel Aviv University, Tel Aviv 69978, Israel*
[b] *Department of Computer Science and Applied Mathematics, Weizmann Institute of Science, Rehovot 76100, Israel*

Received: 8 August 2006 / Accepted: 20 December 2006

Abstract Immunotherapy with *Bacillus Calmette–Guérin* (BCG)—an attenuated strain of *Mycobacterium bovis* (*M. bovis*) used for anti tuberculosis immunization—is a clinically established procedure for the treatment of superficial bladder cancer. However, the mode of action has not yet been fully elucidated, despite much extensive biological experience. The purpose of this paper is to develop a first mathematical model that describes tumor-immune interactions in the bladder as a result of BCG therapy. A mathematical analysis of the ODE model identifies multiple equilibrium points, their stability properties, and bifurcation points. Intriguing regimes of bistability are identified in which treatment has potential to result in a tumor-free equilibrium or a full-blown tumor depending only on initial conditions. Attention is given to estimating parameters and validating the model using published data taken from in vitro, mouse and human studies. The model makes clear that intensity of immunotherapy must be kept in limited bounds. While small treatment levels may fail to clear the tumor, a treatment that is too large can lead to an over-stimulated immune system having dangerous side effects for the patient.

Keywords Bladder cancer · Cytotoxic cells · Immune response · Nonlinear dynamics

1. Introduction

Bladder cancer is a growth of malignant cells initiating in the urinary bladder. The most common neoplasm of the bladder, transitional cell carcinoma (TCC), originates from the transitional epithelium that lines the bladder cavity. It first grows superficially on the inner surface of the bladder as in-situ cancer, expanding from the original site into the adjacent areas. Upon further progression, it invades the bladder wall and vessels, spreading into the neighboring organs as well as systemically forming distant metastases. The treatment

*Corresponding author.
E-mail address: lewi@post.tau.ac.il (Lewi Stone).

of the disease is dependent upon the stage at diagnosis. In the invasive stages, the bladder cancer can only be treated with an aggressive surgery, radiation, and/or chemotherapy (Lamm et al., 2005). However, during the superficial phase the tumor is amenable to local excision, where small regions of cancerous tissue are surgically resected by direct inspection through the urethra, in a procedure called transurethral resection (TUR) (Schenk-Braat and Bangma, 2005). To complete the procedure in the superficial stage, an adjuvant treatment administered into the cavity is generally recommended to destroy any malignant cells that remain following the resection. The two complementary approaches to adjuvant treatment of superficial bladder cancer are the intravesical chemotherapy and the intravesical application of bacillus Calmette–Guérin (BCG) (immunotherapy). Although both adjuvant approaches are practiced clinically, it is generally held that immunotherapy is slightly more effective, is associated with less side effects (Nseyo and Lamm, 1997), and is currently the most frequently applied treatment (Chopin and Gattegno, 2002).

Here we mathematically study the adjuvant immunotherapy of superficial bladder cancer based on the introduction of *Bacillus Calmette–Guérin*—an attenuated strain of *Mycobacterium bovis* (*M. bovis*)—used originally for the treatment of tuberculosis. Bevers et al. (2004) provide a detailed review of the treatment. See also Alexandroff et al. (1999) for a general assessment. Briefly: BCG is introduced into the bladder where it adheres to the damaged regions of the bladder wall. There it primarily infects tumor cells, and to a significantly lesser extent normal cells, and locally stimulates the patient's immune response. This elicits a predominantly confined immune reaction, which mainly targets BCG infected tumor cells and may potentially eliminate the remaining tumor. Thus, the malignant cells are attacked by the patient's own immune system rather than through external chemical or surgical intervention.

BCG is effective in 50–70% of patients (efficacy is defined as disappearance of pathology/symptoms/clinical signs for 5–10 years) with significant reduction in 10 years mortality. However, for a disappointingly high fraction of in-situ patients, the tumor will still recur within this period (Andius and Holmang, 2004). Currently there are no reliable prognostic factors for accurately predicting treatment success (Kim and Steinberg, 2001). The various protocols differ mainly in the frequency of the administration and the dose of the introduced bacillus. The most common protocol is based upon treatment suggested by Morales et al. (1976) and involves weekly instillations of BCG over a 6-week period. Extension of BCG treatment (maintenance immunotherapy) is sometimes used to increase efficacy. BCG treatment side effects include high fever, general malaise and chills, and more rarely persistent bladder infection, BCG induced lung infection, liver toxicity, and BCG sepsis (Kim and Steinberg, 2001). The severe side-effects occur in less then 10% of patients.

It is postulated that the outcome of BCG therapy for the treatment of superficial bladder cancer depends on a complex interaction between the tumor population, the BCG and the immune system (Bevers et al., 2004) as set out in Fig. 1. We believe that these interactions may be better understood by a mathematical model that elucidates the contribution of the various factors in the therapeutic process. The mathematical analysis may illuminate the dominant factors that control the process and that might be externally controlled to improve the outcome. Here we study these interactions by a system of four nonlinear ordinary differential equations that describes the tumor and the immune dynamics for the case of a continued application of BCG therapy. We show that the model exhibits a nontrivial equilibrium structure. Noteworthy, a stable tumor-free equilibrium exists within a

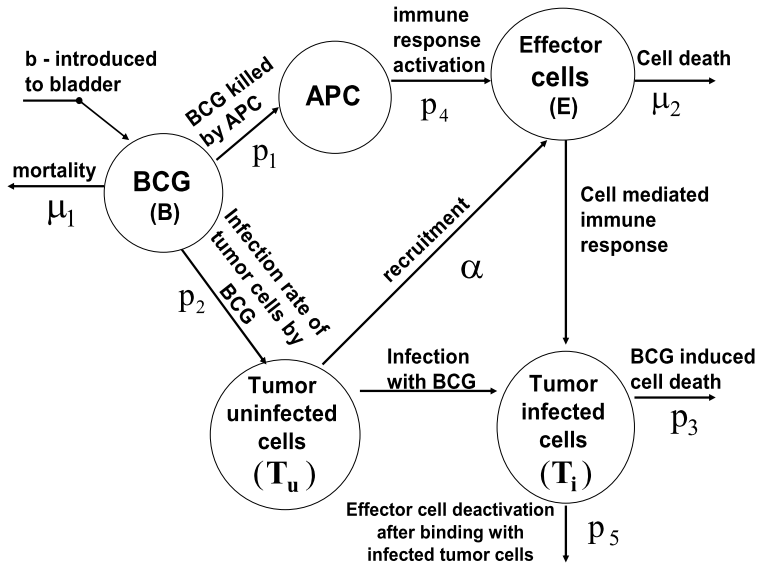

Fig. 1 Schematic view describing interactions between model variables here viewed as compartments. BCG (B) stimulates effector cells (E) of the immune system via APC activation. In addition BCG infects uninfected tumor cells (T_u) which recruit effector cells into the bladder. Infected tumor cells (T_i) are destroyed by effector cells.

biologically feasible parameter regime, and we show the necessary BCG treatment parameters that correspond to tumor eradication. Moreover, we identify regimes of bistability in which a "diseased" tumor laden equilibrium coexists with a "cured" tumor-free equilibrium and where the actual outcome is dependent upon initial conditions (see also Kirschner and Panetta, 1998). The presence of bistability has obvious practical implications for immunotherapy treatment. In addition we discuss more general therapeutic implications.

2. Mathematical model

2.1. Biological framework

The cascade of events leading to BCG-associated tumor cell clearance may be summarized as follows (see Fig. 1):

- *The initial immune response to BCG.* After its instillation in the bladder, BCG (B in Fig. 1) accumulates near the bladder wall, and in superficial tumor cells. In binding to the cell wall, BCG is internalized and processed by both antigen-presenting cells (APC) and uninfected tumor cells denoted by T_u via endocytosis. The "BCG-infected" tumor cells are referred to as T_i.
- *The antitumor effects: the effector cells.* BCG antigens stimulate a strong immune response characterized by a massive appearance of cytokines in the infected areas

and in the urine. The cytokine cascade stemming from the APC activates cytotoxic T cells, lymphocyte-activated killer (Schenk-Braat and Bangma, 2005), natural killer cells (Bohle and Brandau, 2003) and such, which ultimately cause injury to the BCG-infected tumor cells (Patard et al., 1998). For simplicity, we referred to all cells belonging to these different arms of the immune systems as effector cells (E). This targeting of infected tumor cells can lead to elimination of the entire tumor.

2.2. *Formulation of model equations*

We describe the interaction between tumor cells within the bladder, the immune system, and the BCG immunotherapy with a system of nonlinear ODEs. Our modeling approach has similarities to the studies of Kuznetsov et al. (1994), Kirschner and Panetta (1998), De Pillis et al. (2005, 2006) although these authors do not deal with bladder cancer. In our model the tumor cells are divided into two subpopulations; those that have been infected (T_i) with BCG (B) and those that are still uninfected (T_u) and susceptible. As the tumor cells are divided into two pools, the total number of tumor cells is given by: $T = T_i + T_u$.

Since effector cells (E) target and destroy infected tumor cells (T_i) the latter must decrease at an intensity that is proportional to their encounter. By taking random mixing as a first approximation, the encounter rate is proportional to the product $p_3 E T_i$, where p_3 is a rate constant. Similarly, tumor cells become infected with BCG at a rate proportional to the product $p_2 B T_u$ where p_2 is a rate coefficient. Thus the dynamics of the individual pools of tumor populations are:

$$\begin{aligned} \frac{\mathrm{d}T_i}{\mathrm{d}t} &= -p_3 E T_i + p_2 B T_u, \\ \frac{\mathrm{d}T_u}{\mathrm{d}t} &= -p_2 B T_u + \mathrm{G}(T_u). \end{aligned} \tag{1}$$

In the above equations, the number of uninfected tumor cells increase due to the natural growth rate $G(T_u)$ (specified below) of the tumor. Infected tumor cells, on the other hand, contribute little to tumor growth, because BCG has an anti-proliferative effect against human urothelial carcinoma cell lines (Bevers et al., 2004; Bevers, personal communication; Chen et al., 2005).

Typically, BCG is introduced into the bladder cavity by once a week instillations or pulses over a 6-week period. Such processes introduce time dependent discontinuities into the model. The resulting nonautonomous structure can be of considerable analytical complexity, but in some cases can be studied by the method of impulses (Lakshmikantham et al., 1989). At the present stage, we have chosen to simplify the problem by assuming that BCG is introduced into the bladder at a constant rate b, although in a follow up paper we will explore the effects of pulsed therapy. The free BCG binds to malignant urothelial tumor cells, infecting them at a rate p_2 (De Boer et al., 1996; Durek et al., 1999). BCG is lost at the rate p_1 by interaction with macrophages and dendritic cells, and natural killer cells (Wigginton and Kirschner, 2001). To help simplify the model we collectively group the immune cells (APC, natural killer cells, lymphocyte-activated killer) into the single term, effector cells (E). This yields the following equation:

$$\frac{\mathrm{d}B}{\mathrm{d}t} = -\mu_1 B - p_1 E B - p_2 B T_u + b.$$

The term $(-\mu_1)$ is effective net growth rate of BCG and may be viewed as:

$$-\mu_1 = \text{proliferation rate–mortality rate.}$$

For BCG in the bladder, the proliferation rate is negligible (Brandau, private communication); BCG is very slowly growing even in culture. As such, μ_1 reasonably approximates the BCG mortality or decay rate.

The activation of the immune system, which relates to recruitment and maturation of T-killer cells, BCG-activated killers (BAK) are, represented by the following effector cells dynamics:

$$\frac{\mathrm{d}E}{\mathrm{d}t} = -\mu_2 E + \alpha T_i + p_4 E B - p_5 E T_i.$$

Here $p_4 E B$ is the immune response activation that results from the encounter between immune cells and BCG, and controlled by the parameter p_4. Infected tumor cells stimulate recruitment of cytotoxic effector cells from the bone marrow (Bevers et al., 2004) at a rate given by αT_i. The rate of inactivation of E cells via encounter with T_i is given by $p_5 E T_i$, and μ_2 is the natural mortality rate of effector cells.

We arrive at the following system of ordinary differential equations:

$$\begin{aligned}
\frac{\mathrm{d}B}{\mathrm{d}t} &= -\mu_1 B - p_1 E B - p_2 B T_u + b,\\
\frac{\mathrm{d}E}{\mathrm{d}t} &= -\mu_2 E + \alpha T_i + p_4 E B - p_5 E T_i,\\
\frac{\mathrm{d}T_i}{\mathrm{d}t} &= -p_3 E T_i + p_2 B T_u,\\
\frac{\mathrm{d}T_u}{\mathrm{d}t} &= -p_2 B T_u + G(T_u).
\end{aligned} \tag{2}$$

2.3. The tumor growth rates

In this study we compare two functional forms for the per-capita growth rate of the tumor $G(T_u)$:

(a) *The logistic model*, in which the tumor growth is given by:

$$G(T_u) = r(1 - \beta T_u)T_u, \tag{3a}$$

where r is the growth rate of tumor cells, and β is the death of tumor cells as a result of self-limiting competition for resources such as oxygen and glucose. β^{-1} may be viewed as the maximum carrying capacity of the tumor under logistic growth.

(b) *The exponential model* with tumor growth:

$$G(T_u) = r T_u \tag{3b}$$

with r a constant. This describes an exponentially increasing tumor mass. Note that the exponential model is a special case of the logistic model for which $\beta = 0$.

The well known Gompertz law (Banks, 1994) is also a potentially useful functional growth rate form. However, given the latter's similarities to the logistic equation, it is unlikely to make qualitative differences to the main results found here.

2.4. *Scaling of parameters*

The system (2) and (3a), (3b) may be placed in dimensionless form, using the following scaling:

$$B' = \frac{B}{B_0}, \qquad E' = \frac{E}{E_0}, \qquad T_i' = \frac{T_i}{T_{i_0}}, \qquad T_u' = \frac{T_u}{T_{u_0}}, \qquad t' = \mu_1 t,$$
$$b' = \frac{b}{\mu_1 B_0}, \qquad \beta' = \beta T_{u_0}, \qquad \alpha = \frac{\alpha}{\mu_1}, \qquad r' = \frac{r}{\mu_1}, \qquad \mu = \frac{\mu_2}{\mu_1},$$
$$p_1' = \frac{p_1}{\mu_1} E_0, \qquad p_2' = \frac{p_2}{\mu_1} T_{u_0}, \qquad p_3' = \frac{p_3}{\mu_1} E_0, \qquad p_4' = \frac{p_4}{\mu_1} B_0,$$
$$p_5' = \frac{p_5}{\mu_1} T_{i_0}.$$

The parameters p_1, and p_2 may be eliminated by choosing the additional scaling:

$$B_0 = T_{i_0} = T_{u_0} = \frac{\mu_1}{p_2} \quad \text{and} \quad E_0 = \frac{\mu_1}{p_1}.$$

In practice, there is a trade off between reducing parameters and retaining parameters that have operational meaning. For these reasons we choose the scaling $|B_0| = |E_0| = |T_{i_0}| = |T_{u_0}| = 10^6$ cells (similar to Kuznetsov et al., 1994), which ensures that the model is in dimensionless form, but retains most of the original parameters. Dropping the prime notation for convenience, we obtain the final form of the model equations here specified with logistic tumor growth:

$$\begin{aligned}
\frac{\mathrm{d}B}{\mathrm{d}t} &= B(-1 - p_1 E - p_2 T_u) + b, \\
\frac{\mathrm{d}E}{\mathrm{d}t} &= E(-\mu + p_4 B - p_5 T_i) + \alpha T_i, \\
\frac{\mathrm{d}T_i}{\mathrm{d}t} &= -p_3 E T_i + p_2 B T_u, \\
\frac{\mathrm{d}T_u}{\mathrm{d}t} &= T_u\big(-p_2 B + r[1 - \beta T_u]\big),
\end{aligned} \tag{4}$$

where all parameters are positive. Again, the exponential growth model is retrieved by setting $\beta = 0$.

2.5. *Model parameters*

To complete the mathematical model it is useful to estimate parameter ranges that are realistic and agree with values reported in the literature. Although this plays some role

in the analysis that follows, we emphasise that our goal here is not to derive a predictive simulation model using exact rate parameters. Instead, we aim to find generic qualitative results that are intrinsic to the model's structure. As our analytical results are not tied to any specific growth rates, we do not require precise rate values. This notwithstanding, parameter values are compiled from peer-reviewed mathematical models of cancer growth and immunotherapy, and in many cases we have attempted to improve these estimates. A summary of the parameter values used in this paper is given in Table 1. In this section we briefly discuss the acquisition of the parameters of the unscaled model (2) i.e., before nondimensionalization.

The natural mortality rate of BCG μ_1 was estimated from experimental data given in the study of Archuleta et al. (2002). Figure 2a shows the mortality rate of the *Mycobacterium avium (M. avium)* strain, similar to *M. bovis* (both are slow growing). The BCG decay rate is exponential (linear on a logarithmic scale) over the first $\tau = 10$ days and estimated as $\mu_1 = \ln \frac{10^7}{2\times 10^5} = 0.16$ cells/day in that period. The decay then decelerated and was calculated as $\mu_1 = 0.07$ over the first 23 days. Over a 50 day period, the decay was $\mu_1 = 0.04$. For the model, a rough average of these values seemed a reasonable first estimate for the decay rate and we thus set $\mu_1 = 0.1$ in our simulations, corresponding to half life for *M. avium* of 7 days ($\tau_{0.5} = \ln 2/\mu_1 = 7$).

Typical values for the BCG instillation b were obtained from the clinical data of Cheng et al. (2004) in which patients received weekly BCG doses corresponding to 2.2×10^8–6.4×10^8 c.f.u.'s (colony-forming units, i.e., number of viable bacterial cells). Most of this leaves the bladder within the first two hours of instillation. Brandau (personal communication) estimates that 99% of the BCG is lost this way. A reasonable daily rate for b is thus in the range $0.01 \times (2.2 \times 10^8$–$6.4 \times 10^8)/7$ days $= 3 \times 10^5$–10×10^5 c.f.u./day.

Many studies report estimates of the parameters r and β (3a), (3b) describing the tumor's logistic or exponential growth (see summary in Table 1). Kuznetsov et al. (1994) used an estimate of $r = 0.18$ days^{-1} and De Pillis et al. (2005) used $r = 0.51$ days^{-1}, for the growth rate r which translate to very fast doubling times of approximately 1–4 days. The data of Aranha et al. (2000) in Fig. 2b is compatible with bladder cancer in vitro growth rates of $r \sim 0.37$–0.5 days^{-1} with a doubling time of approximately 1.5–2 days. We suspect that these large growth rates may be biased as they represent cell growth in vitro in favorable medium without the constrains that normally exist in the tissue. On the other hand, the in vivo studies in the medical literature report growth rates of r that equal 0.001–0.03 days^{-1} for breast cancer (Spratt et al., 1993; Shochat et al., 1999). Here we assume that the in vivo rates of bladder cancer growth are an order of magnitude slower than in vitro and approximate r to be in the range $r = 0.01$–0.045 days^{-1} for our simulations.

Under logistic growth, the parameter β is estimated by noting that the maximum carrying capacity of the tumor is $T_u = \beta^{-1}$ cells. Lämmle et al. (2002) give information regarding the sizes of bladder cancer, as determined by MR imaging. They report tumor sizes ranging from 2–32 mm in radius. From this, we calculated the maximal tumor surface area assuming it being circular in shape. It was also assumed that the tumor is some 3 cells deep allowing the volume to be determined based on the length of cell being approximately 10 μm. Given that 1 mm$^3 \sim 10^6$ cells (Spratt et al., 1993), the number of tumor cells is:

$$\beta^{-1} = \pi r^2 h \times 10^6 \approx \pi \times 32^2 \times 3 \times 10^{-2} \times 10^6 = 0.9 \times 10^8 \text{ cells},$$

Table 1 List of all parameters (E—calculated for exponential model, L—calculated for logistic model, H—for human data). Note that dimensionless estimates are obtained from source values using transformations given in Section 2.4

Par.	Description	Units	Source value	Dimensionless estimate	Source
μ_1	The rate of BCG decay	$t^{-1} = \text{days}^{-1}$	0.1	1	Archuleta et al., 2002
μ_2	Effector cells mortality rate	$t^{-1} = \text{days}^{-1}$	0.041	0.41	Kuznetsov et al., 1994
p_1	The rate of BCG killed by APC	$\text{cells}^{-1}\,\text{days}^{-1}$	1.25×10^{-7}	1.25	Wigginton and Kirschner, 2001
p_2	Infection rate of tumor cells by BCG	$\cdots$	0.285×10^{-7}	0.285	Not found
p_3	Rate of destruction of infected tumor cells by effector cells	$\cdots$	1.1×10^{-7}	1.1	Kuznetsov et al., 1994
p_4	Immune response activation rate	$\cdots$	0.12×10^{-7}	0	Not found
p_5	Rate of E deactivation after binding with infected tumor cells	$\cdots$	3.45×10^{-10}	0.003	Kuznetsov et al., 1994
α	Rate of E stimulation due to infected tumor cells	$t^{-1} = \text{days}^{-1}$	0.052	0.52	Wigginton and Kirschner, 2001
β	$1/\beta =$ tumor carrying capacity	cells^{-1}	0.11×10^{-7}	0.011	Lämmle et al., 2002;
			2×10^{-8}	0.02 Range used: 0.013–0.022	De Pillis et al., 2006
r	Tumor growth rate	$t^{-1} = \text{days}^{-1}$	0.0032 (L)–H 0.18 (L)-mice 0.0033(E)–H 0.37—in vitro 0.012 (E)	0.032 1.8 0.033 3.7 0.12	Spratt et al., 1993 Kuznetsov et al., 1994 Shochat et al., 1999 Aranha et al., 2000 Swanson et al., 2003
			Range used*: 0.01–0.045 (L) 0.0028 (E)	Range used*: 0.1–0.45 (L) 0.028 (E)	
b	Bio-effective concentration of BCG	c.f.u./day	3×10^5–1×10^6	3–10 Range used: 0–10	Cheng et al., 2004

*Marks ranges of parameters used in all figures except Fig. 9 which explores large changes in growth rate r

and thus $\beta = 0.11 \times 10^{-7}$.

Where possible, our estimates of the parameters in the immunological response ($\mu_2, p_1, p_3, p_5, \alpha$) are based on the works of Kuznetsov et al. (1994), Kirschner and

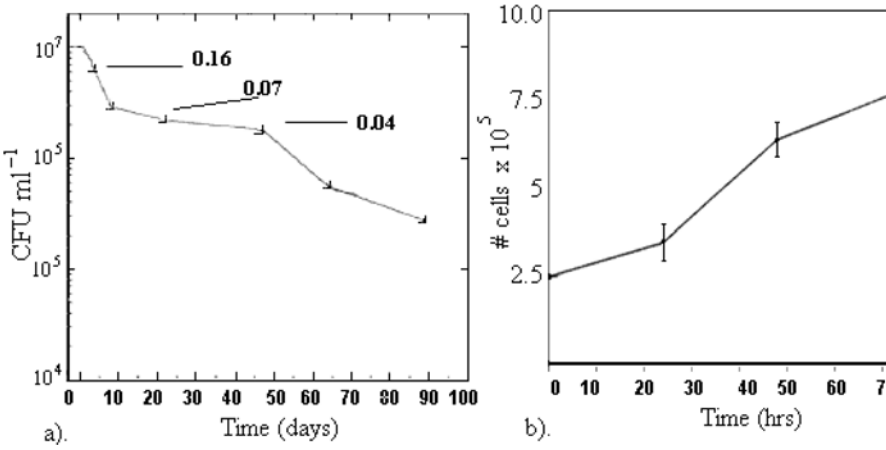

Fig. 2 (a) Viability of M. avium during starvation in water in temperature 37°C from Archuleta et al. (2002). Each point represents the mean and standard deviation of *M. avium* (c.f.u.'s) in a minimum of three plates. Since log viability does not fall linearly, the decay is not exactly exponential. The decay μ_1 is determined by calculations over several different time windows (see text); the results are displayed on the graph. (b) The graph shows tumor cell growth of HTB9 cells in vitro (TCC human lines, grade II) from Aranha et al. (2000). The number of living cells is plotted against incubation time.

Panetta (1998) and Wigginton and Kirschner (2001), although some of the variables used there are rough estimates. The parameter p_2 was estimated by imposing reasonable time scales to the process of tumor eradication (several weeks) in simulations. Due to the highly non-trivial nature of the multidimensional parameter estimation and its nonuniqueness (Press et al., 1992), some of the values chosen here should be viewed as at least reasonable order-of-magnitude indicators. Table 1 lists each parameter, its baseline value, and source. Note that dimensionless estimates are obtained from source values using transformations given in Section 2.4.

3. Model analysis

3.1. Invariance of positive orthant

Assume that the model begins with positive initial conditions:

$$B(0) > 0, \qquad E(0) > 0, \qquad T_i(0) > 0, \qquad T_u(0) > 0.$$

The following elementary considerations show that trajectories of model equations (4) must then remain in the positive orthant (R^4_+) for all time, i.e. the region is invariant. This is based on the following observations. From (4), if $b > 0$ then when $B = 0$, $\mathrm{d}B/\mathrm{d}t = b > 0$ and it follows that $B(t) > 0$ for all t (given that $B(0) > 0$). If $b = 0$, then: $B(t) = B(0)\exp(-\int_0^t [1 + p_1 E + p_2 T_u]\,\mathrm{d}t) > 0$, if $B(0) > 0$. Likewise, $T_u(t) > 0$ for all t if $T_u(0) > 0$. Since $B(t) > 0$ and $T_u(t) > 0$, then $\mathrm{d}T_i/\mathrm{d}t = p_2 B T_u > 0$ when $T_i = 0$, and thus $T_i(t) > 0$ for all t. Now when $E = 0$, $\mathrm{d}E/\mathrm{d}t = \alpha T_i > 0$, implying that $E(t) > 0$ for all t.

Thus the positive orthant R_+^4 is invariant and $B(t) > 0$, $E(t) > 0$, $T_i(t) > 0$, $T_u(t) > 0$ for all t. We use this property in the section that follows.

3.2. *Equilibrium and stability analysis*

The equilibria of the model (4) are found by setting all derivatives to zero and solving for B^*, E^*, T_i^* and T_u^*, with the star notation indicating the variables are at their equilibrium values. Equations (4) have multiple equilibria but, given the invariance of the positive orthant, we need only focus on the nonnegative equilibria assuming all initial conditions are positive.

When analyzing the stability of each equilibrium of the above nonlinear system, one examines the Jacobian:

$$J = \begin{bmatrix} -1 - p_2 T_u^* - p_1 E^* & -p_1 B^* & 0 & -p_2 B^* \\ p_1 E^* & -\mu + p_4 B^* - p_5 T_i^* & \alpha - E^* p_5 & 0 \\ p_2 T_u^* & -p_3 T_i^* & -p_3 E^* & p_2 B^* \\ -p_2 T_u^* & 0 & 0 & -p_2 B + r - 2r\beta T_u^* \end{bmatrix}. \tag{5}$$

Let the eigenvalues of the Jacobian examined at a particular equilibrium be $\overline{\lambda} = [\lambda_1, \lambda_2, \lambda_3, \lambda_4]$ and set

$$\Lambda = \max_i \{\mathrm{Re}(\lambda_i)\}.$$

If $\Lambda < 0$, then all eigenvalues must have negative real parts and the equilibrium is locally stable.

The following sections provide a stability analysis of the model's nonnegative equilibria, first in the absence of immunotherapy (Section 3.3) and second under conditions of continuous therapy (Section 3.4).

3.3. *Absence of BCG treatment ($b = 0$)*

The model (4) in the absence of therapy ($b = 0$) is characterized by two different types of equilibria that are summarized in Table 2.

Table 2 Summary of the stability characteristics for the nonnegative equilibria solutions of system (4) in the absence of therapy ($b = 0$). The tumor-free equilibrium E_1 is common to both exponential (E) and logistic (L) growth models whereas the tumor-equilibrium E_2 exists only for the logistic model. The exponential model lacks any stable equilibrium

$b = 0$	B^*	E^*	T_i^*	T_u^*	Stability
E_1 (L&E)	0	0	0	0	Tumor-free equilibrium—always unstable
E_2 (L)	0	0	0	$\frac{1}{\beta}$	Tumor equilibrium—Liapunov stable

3.3.1. The tumor-free equilibrium

$$E_1: \quad B^* = E^* = T_i^* = T_u^* = 0,$$

which exists in both the logistic and exponential models.

Stability: The eigenvalues of the Jacobian (5) evaluated at equilibrium are: $\overline{\lambda} = [-1, -\mu, 0, r]$ for both models. Since $\Lambda = \max_i\{\mathrm{Re}(\lambda_i)\} = r > 0$, one eigenvalue is always positive and the tumor free equilibrium is an unstable saddle point for all parameters. The eigenvector of the Jacobian corresponding to the eigenvalue $\lambda = r$ is easily found to be $\overline{e} = [0, 0, 0, 1]$. This refers to a state dominated by the tumor's exponential growth: $\mathrm{d}T_u/\mathrm{d}t = rT_u$ or $T_u(t) = T_u(0)\exp(rt)$.

3.3.2. The tumor equilibrium (logistic model)

$$E_2: \quad B^* = E^* = T_i^* = 0, \quad T_u^* = \frac{1}{\beta}.$$

The logistic model ($\beta > 0$) exhibits a second nonnegative equilibrium that corresponds to a state where the tumor reaches its full scale carrying capacity $T_u^* = \frac{1}{\beta}$. (This equilibrium does not exist in the exponential model ($\beta = 0$).) At the equilibrium, effector cells are absent ($E^* = 0$) because there is no infection to stimulate the immune system. With the immune system "switched off" there is no resistance to tumor growth.

Stability: The eigenvalues of the Jacobian at this equilibrium are:

$$\overline{\lambda} = \left[-\frac{p_2 + \beta}{\beta}, -\mu, 0, -r\right]. \tag{6}$$

The zero eigenvalue in (6) indicates that the equilibrium is characterized by neutral stability. However, numerical simulations indicate that the equilibrium is locally stable (see Fig. 3). This is a case where the linearized dynamics fail to represent the true dynamics of the nonlinear system due to the presence of a zero eigenvalue. Nevertheless, it is possible to show that the equilibrium is in fact Liapunov stable for initial conditions in R_+^4 (see Appendix A).

3.4. Continuous BCG immunotherapy ($b > 0$)

The constant BCG immunotherapy is a treatment program that introduces a continuous antigenic stimulus. With constant BCG immunotherapy treatment ($b > 0$) both the logistic and exponential models have three distinct types of equilibria, are summarized in Table 3, denoted here as the "tumor-free" equilibrium E_1^b, the "side-effect" equilibrium E_2^b and the "tumor" equilibrium E_3^b.

3.4.1. Tumor-free equilibrium (logistic and exponential)

$$E_1^b: \quad B^* = b, \qquad E^* = T_i^* = T_u^* = 0.$$

Stability: Substituting E_1^b into the Jacobian (5), a calculation yields the following eigenvalues:

$$\overline{\lambda} = [-1; -\mu + p_4 b; 0; -p_2 b + r].$$

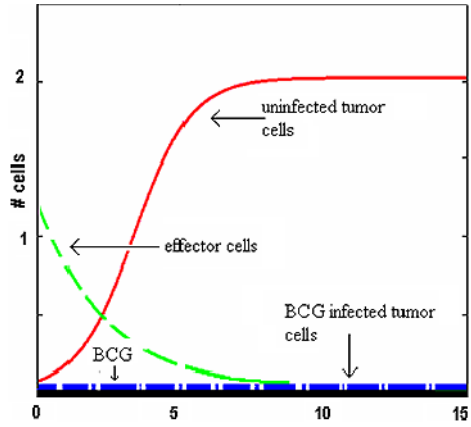

Fig. 3 Numerical simulation of trajectories of (4) with logistic growth rate as they are attracted to the tumor equilibrium E_2. The graph shows the evolution in time (days) to equilibrium of T_u (uninfected tumor cells, solid line), E (effector cells, dashed line), T_i (tumor cells infected with BCG, dash-dotted line) and B (BCG, solid heavy line). The tumor cells eventually reach their maximum carrying capacity $T_u^* = 1/\beta = 0.2$. Parameters as in Table 1, with $\beta = 5$ (for demonstration); $r = 0.12$; $b = 0$.

Table 3 Summary of the stability conditions for the nonnegative equilibria solutions of system (4) under immunotherapy ($b > 0$). The tumor-free equilibria E_1^b and E_2^b are identical for both exponential (E) and logistic (L) growth models. The parameter ranges for which the equilibria are stable are given in right-hand column

$b > 0$	B^*	E^*	T_i^*	T_u^*	Stability
E_1^b (E&L)	b	0	0	0	$\frac{r}{p_2} < b < \frac{\mu}{p_4}$ locally stable
E_2^b (E&L)	$\frac{\mu}{p_4}$	$\frac{bp_4}{\mu p_1} - \frac{1}{p_1}$	0	0	$\frac{r}{p_2} < \frac{\mu}{p_4} < b$ locally stable
E_3^b (E)	>0	>0	>0	>0	If exists, always unstable (numerical simulations)
E_3^b (L)	>0	>0	>0	>0	If exists, always Locally Stable (numerical simulations)

Apart from $\lambda_3 = 0$, all eigenvalues are negative if:

$$\frac{r}{p_2} < b < \frac{\mu}{p_4}. \tag{7}$$

The zero eigenvalue indicates that the system will be neutrally stable in this parameter range, yet simulations indicate local stability. As the numerical simulations in Fig. 4 show, the tumor rapidly disappears if the BCG influx rate b satisfies the criteria given in (7). Although we are unable to provide a rigorous stability analysis of this equilibrium ($b > 0$), it is possible to sketch the principle processes that give rise to local stability despite the zero eigenvalue. A linear analysis of (4) in a neighborhood of this equilibrium shows that for $B \to B^* = b$ and $T_u \to T_u^* = 0$ as $t \to \infty$. Equation (4) can now be simplified to almost the same reduced system (6) which was found to be Liapunov stable.

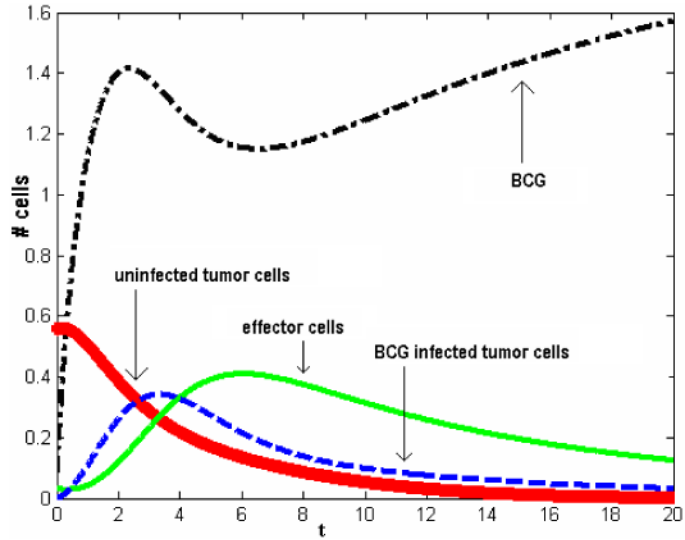

Fig. 4 Numerical simulation of (4) with logistic growth rate for $b > 0$. The tumor-free equilibrium E_1^b is locally stable. The graph shows the evolution in time to equilibrium of uninfected tumor cells (solid heavy line), effector cells (solid line), tumor cells infected with BCG (dashed line) and BCG (dash-dotted line). Parameters as in Table 1, with: $\beta = 0.0155$; $r = 0.12$; $b = 1.9$. Note that in the present scaling each time unit is equivalent to 10 days. Faster tumor eradication may be obtained by increasing the tumor infection rate p_2. For example, $p_2 = 2.3$ corresponds to large scale tumor eradication within 1–2 weeks.

The criterion given in (7) gives the ranges for which constant BCG treatment is able to clear the tumor to a point where the immune system response is no longer required ($E^* = 0$). An intuitive understanding of the breakpoints of this range may be gained as follows. The left-hand side breakpoint (in (7)) corresponds to the point where $r = bp_2$. At equilibrium, the term bp_2 is the per-capita infection rate of the tumor. Thus we see that when this infection rate is greater (although not too much greater) than the tumor growth rate r, the tumor-free equilibrium is stable. For smaller infection rates, the tumor's growth rate dominates and the tumor-free equilibrium *destabilizes*. The right hand breakpoint occurs when $\mu = bp_4$, which at equilibrium, is the per-capita rate of stimulation of the effector cells by bacteria. When this stimulation rate is less than the effector cells own mortality rate μ, the tumor-free equilibrium is stable. Should it be larger, effector cells are over-stimulated and the equilibrium loses stability.

It is of interest to identify those factors, which stabilize the desired tumor-free equilibrium state:

1. The rate of BCG treatment (b) is relatively large compared to the tumor growth rate (r).
2. The BCG infection rate of the tumor (p_2) is relatively large and the treatment is effective by "brute force".
3. The immune system activation (p_4) is not strong enough to provoke a side-effect reaction ($E^* > 0$, see below).

It is noteworthy that the tumor dynamics linearized about the equilibrium may be approximated as $\frac{dT_u}{dt} = (-p_2 b + r)T_u$. The solution of the equation is:

$$T_u(t) = T_u(0)\exp\big[(-p_2 b + r)t\big], \tag{8}$$

which decreases exponentially to zero when the equilibrium is stable $[(-p_2 b + r) < 0]$. This shows that with the application of immunotherapy, the tumor will retreat at a rate that can be controlled by the intensity of treatment b.

3.4.2. "Side effect" equilibrium E_2^b (logistic and exponential)

$$E_2^b: \quad B^* = \frac{\mu}{p_4} > 0, \qquad E^* = \frac{bp_4}{\mu p_1} - \frac{1}{p_1} > 0, \qquad T_i^* = T_u^* = 0.$$

The equilibrium is characterized by a permanent over-stimulated immune system. Before BCG therapy only low numbers of leukocytes can be detected in the bladder. After repeated BCG instillation, the influx of different types of effector cells (macrophages, lymphocytes) that aim to kill cells infected with BCG is observed (Bohle and Brandau, 2003). Often this transient behavior subsides with time (de Reijke et al., 1999). Occasionally however, BCG may invoke a widespread immune response. This in turn may cause troubling systemic side effects: high fever, malaise and rarely an immune related lung inflammation (Elkabani et al., 2000). These side effects are considered features to be associated with equilibrium E_2^b and may be permanent.

Stability: The eigenvalues of the Jacobian matrix are:

$$\overline{\lambda} = \left[\frac{p_3(\mu - bp_4)}{\mu p_1}, \frac{-\mu p_2 + r p_4}{p_1}, \frac{1}{2}\frac{-bp_4 \pm \sqrt{b^2 p_4^2 + 4\mu^3 - 4bp_4\mu^2}}{\mu}\right].$$

Manipulation of the expressions for the eigenvalues shows that the equilibrium is nonnegative and locally stable with all eigenvalues having negative real parts if:

$$\frac{r}{p_2} < \frac{\mu}{p_4} < b, \tag{9}$$

where the right hand side inequality ($\frac{\mu}{p_4} < b$) is simply an appearance of the condition that $E^* > 0$. Interestingly, (7) shows that in the regime in which E_2^b is stable (9), the tumor free equilibrium E_1^b is unstable and vice-versa. Thus there is a transcritical bifurcation at the point $b = \frac{\mu}{p_4}$ which separates the regimes of stability between the two equilibria. From (7) and (9) it is evident that E_1^b and E_2^b will be stable when the tumor growth rate (r) is sufficiently smaller than $r_{\text{crit}} = \mu p_2 / p_4$.

3.4.3. Tumor equilibrium E_3^b (logistic and exponential)

This equilibrium is characterized by all populations having positive equilibrium values:

$$B^* > 0, \qquad E^* > 0, \qquad T_i^* > 0, \qquad T_u^* > 0$$

where

$$B^* = \frac{(1-\beta T_u^*)r}{p_2}, \qquad E^* = \frac{p_2 B^* T_u^*}{p_3 T_i^*},$$
$$T_i^* = \frac{p_1(1-\beta T_u^*)^2 r^2 T_u^*}{p_3(bp_2 + r(1-\beta T_u^*)(1-p_2 T_u^*))} \tag{10}$$

and T_u^* is a real positive root of a fifth-order polynomial.

(a) *Equilibrium E_3^b for logistic growth rate ($\beta > 0$)*: Simple precise stability criteria for equilibrium E_3^b are not obtainable analytically. However, numerical studies (e.g., see region III in Fig. 9a) indicate that a sufficient (but not necessary) condition for the equilibrium to be stable is that both the tumor-free and the "side-effect" equilibria (E_1^b and E_2^b) are unstable. That is when the tumor growth rate (r) is sufficiently large with $r > r_{\text{crit}} = \mu p_2 / p_4$.

(b) *Equilibrium E_3^b for exponential growth rate ($\beta = 0$)*: Expressions (10) for exponential growth rate become:

$$B^* = \frac{r}{p_2}, \qquad E^* = \frac{r T_u^*}{p_3 T_i^*}, \qquad T_u^* = \frac{(bp_2 - r)p_3 T_i^*}{r(p_2 p_3 T_i^* + r p_1)},$$

$$T_i^* = \frac{1}{2\alpha p_2 p_3}\Big[-\alpha p_1 r - r p_5 + b p_2 p_5$$
$$\pm \sqrt{(-\alpha p_1 r - r p_5 + b p_2 p_5)^2 + 4\alpha p_3\big(\mu b p_2^2 - p_2 p_4 b r + p_4 r^2 - p_2 r \mu\big)}\Big].$$

For T_i^* to have a positive solution it is essential that: $(r - p_2 b)(r - \frac{\mu}{p_4} p_2) > 0$. This last criterion expression will be satisfied only when: $r < \min\{p_2 b; \frac{p_2}{p_4}\mu\}$, assuming that $T_u^* > 0$. However, from numerical simulations (e.g., Fig. 5) E_3^b is always unstable.

4. Immunotherapy control of equilibrium structure and bistability

In order to characterize the effects of immunotherapy, bifurcation diagrams are calculated for each model as a function of BCG intensity (b). For the exponential model, Fig. 5 shows that for low levels of immunotherapy ($b < r/p_2$) the equilibria E_1^b and E_2^b equilibria are unstable (equilibrium E_3^b does not exist). The tumor grows exponentially in size as shown in Section 3.3.1. Low levels of immunotherapy are thus ineffective. At intermediate levels of treatment ($r/p_2 < b < \mu/p_4$), the tumor-free equilibrium E_1^b is stable and tumor cure is possible. When $b > \mu/p_4$, the side-effect equilibrium E_2^b stabilizes and is the only stable equilibrium. In this regime, although the tumor is eradicated, the treatment level is so strong that the immune system remains active, and E^* increases with b (Lamm et al., 2005). Note that under more intense treatment levels ($b > r/p_2$), E_3^b exists, but is not stable.

Figures 6 and 7, show that the logistic version of the model has the same qualitative features. There are, however, noteworthy differences. At low levels of immunotherapy the model attains a stable equilibrium where the tumor reaches a fixed finite size rather

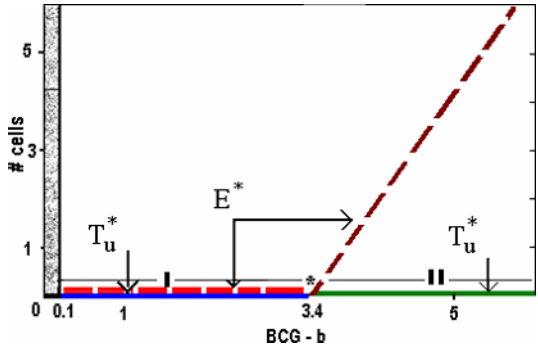

Fig. 5 Equilibrium transitions for exponential model as a function of BCG immunotherapy rate b. The graph shows equilibrium of uninfected tumor cells (solid line) and effector cells (dashed line). For $b < r/p_2 = 0.1$ (shaded region to left of vertical black line) E_1^b and E_2^b are unstable, while E_3^b does not exist. For $r/p_2 < b < \mu/p_4 = 3.4$, the tumor free equilibrium E_1^b (I) is stable, E_3^b exists but is unstable. When $b > \mu/p_4 = 3.4$, E_2^b (II) is stable, E_3^b exists but is unstable. Parameters as in Table 1 with $\beta = 0$; $r = 0.028$.

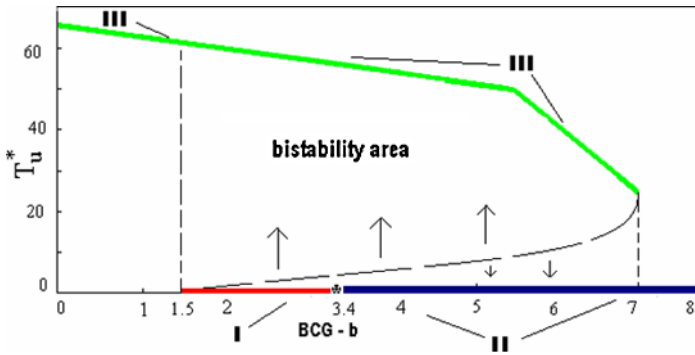

Fig. 6 Bifurcation diagram of the logistic version of the model plotting uninfected tumor cells (T_u^*) as a function of BCG immunotherapy rate (b). When $b < r/p_2 = 1.5$, the tumor equilibrium E_3^b (III) is stable. When $r/p_2 = 1.5 < b < \mu/p_4 = 3.4$, the tumor free equilibrium E_1^b (I) and tumor equilibrium are stable E_3^b (III). When $3.4 < b < 7.2$, both the side effect equilibrium E_2^b (II) and the tumor equilibrium E_3^b (III) are stable. At higher levels of immunotherapy ($b > \mu/p_4 = 3.4$) only the side effect equilibrium E_2^b (II) is stable. Parameters as in Table 1, with: $\beta = 0.0155$; $r = 0.43$.

than unstable exponential growth. At intermediate levels of therapy there is a region of bistability in which E_3^b, the tumor equilibrium coexists with either E_1^b or E_2^b (both tumor-free). In this regime, the equilibrium that is eventually reached depends solely on the initial conditions. In the range $1.5 < b < 7$, tumors whose size are above the critical line shown in Fig. 6 will be attracted to the tumor equilibrium while tumors below this line will be attracted to the tumor-free equilibrium. This means that the outcome of the immunotherapy can depend critically on the given state of the tumor. If the tumor is eradicated at relatively high levels of immunotherapy ($b > \mu/p_4 = 3.4$), this corresponds to the side-effect equilibrium E_2^b.

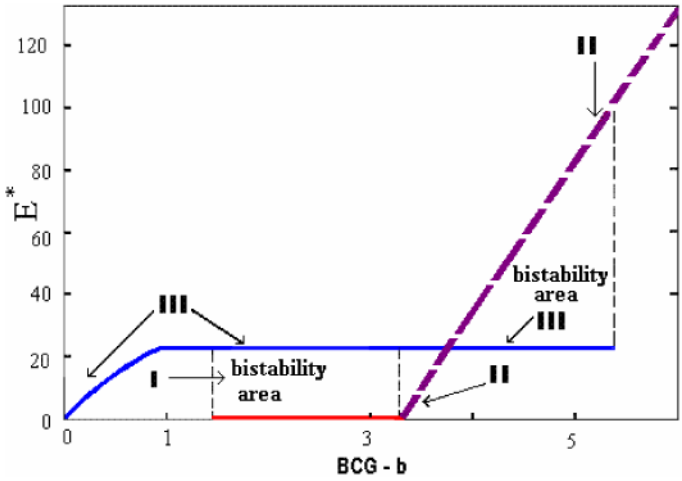

Fig. 7 Bifurcation diagram of the logistic version of the model plotting effector cells (E^*) as a function of BCG immunotherapy rate (b). At low levels of immunotherapy ($b < r/p_2 = 1.5$) the tumor equilibrium E_3^b (III) is stable. At intermediate levels there is a regime of bistability. At high levels of immunotherapy ($b > \mu/p_4 = 3.4$) the side effect equilibrium E_2^b (II) is stable. Parameters are as in Fig. 6.

Figure 8 helps visualize the bistability effect. A set of trajectories that are solutions of (4) is plotted in the phase space $B(t)$ vs. $T_u(t)$. The phase space can be divided into two regions: below the separatrix line where every trajectory converges to E_1^b and above the separatrix where all trajectories converge to E_3^b. The separatrix indicates the critical initial conditions that determine if the BCG treatment will eradicate the tumor or not.

The bifurcation diagram of Fig. 9a explores the effect of the tumor growth rate (r) on tumor equilibrium levels $T_u(t)$. Note that the level of BCG dose treatment is taken to be above the critical level ($b = 3.6 > \mu/p_4 = 3.4$) which ensures that the tumor-free equilibrium E_1^b is unstable. When the intrinsic growth rate $r < r_{\text{crit}} = \mu p_2/p_4 = 0.96$ the side-effect equilibrium E_2^b (II) is stable and unstable otherwise. Note that there is a regime of bistability ($0.19 < r < 0.96$) where both the tumor equilibrium (E_3^b) and the side-effect equilibrium (E_2^b) coexist and are stable. For $r > r_{\text{crit}}$, only equilibrium E_3^b exists and it is stable.

Interestingly, for large tumor growth rates $r > r_{\text{crit}}$, the tumor-equilibrium E_3^b is extremely robust and is stable independent of the amount of immunotherapy b. With $r = 1.1$, for example, Fig. 9b plots the tumor equilibrium until $b = 45$ although the same trend is found for enormous doses of therapy beyond $b = 1{,}000$. That is, no amount of immunotherapy can eradicate the model-tumor in this regime. In order to help elucidate this feature, for the given parameter ranges, it is possible to approximate E_3^b with good accuracy as:

$$B^* = \frac{\mu}{p_4}, \qquad E^* = \frac{1}{p_1}\left(\frac{bp_4}{\mu} - \frac{p_2}{\beta} + \frac{\mu p_2^2}{\beta r p_4} - 1\right),$$

$$T_i^* = \frac{p_2}{p_3}\frac{B^* T_u^*}{E^*}, \qquad T_u^* = \frac{1}{\beta}\left(1 - \frac{\mu p_2}{r p_4}\right).$$

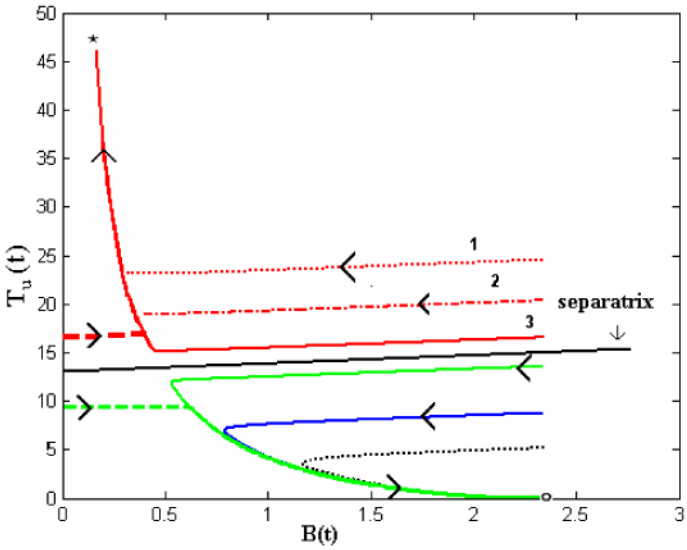

Fig. 8 Phase portrait indicating bistability and dependence on initial conditions. The three trajectories (1–3) above the separatrix converge to the tumor-equilibrium E_3^b (symbol $*$). The three trajectories below the separatrix converge to the tumor-free equilibrium E_1^b (symbol $\circ$). All model simulations have parameters as in Table 1, with in $b = 2.4$; $\beta = 0.0155$; $r = 0.43$. All numerical simulations are performed with fixed initial conditions for B, E and T_i.

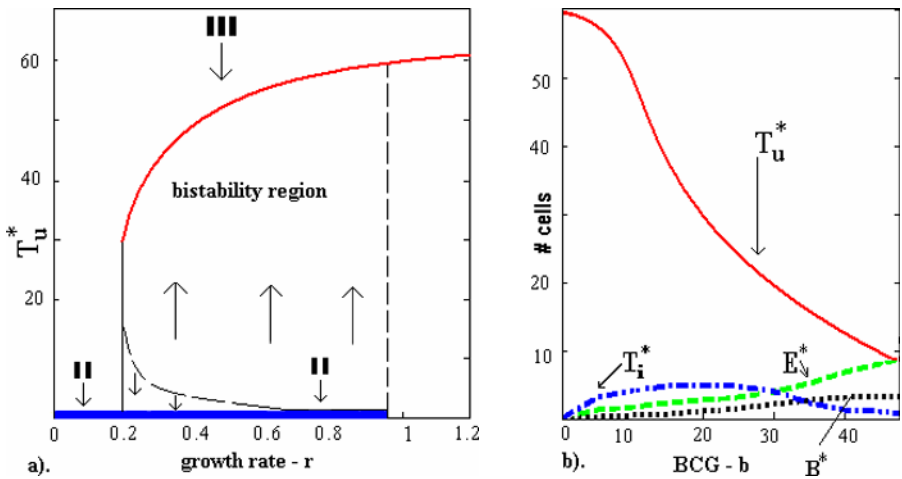

Fig. 9 (a) Bifurcation diagram of the logistic version of the model where the equilibrium number of uninfected tumor cells T_u^* is plotted as a function of the tumor's intrinsic growth rate (r) for a fixed value of immunotherapy $b = 3.6$ ($b > \mu/p_4 = 3.4$). In the latter regime, only the two equilibria E_2^b (II) and E_3^b (III) can exist. Bistability is apparent. Parameters as in Fig. 6, with $b = 3.6$ and varying value of r. (b) Equilibrium values of all model variables plotted as a function of BCG immunotherapy rate b at fixed level of tumor growth $r = 1.1 > r_{\text{crit}}$. Parameters as in Fig. 6. The tumor is maintained no matter how large the immunotherapy applied.

This reveals that B^* and T_u^* are indeed independent of the intensity of immunotherapy b, while E^* increases linearly. In this regime, the infected tumor cells T_i^* are found to be relatively small in number ($T_i^* \sim 0.8$). The processes promoting this behavior may be understood as follows. The high levels of therapy do not enhance net BCG equilibrium concentration. Instead the BCG flux turns-over rapidly and is mostly taken up and shunted through to the effector cell population boosting the equilibrium E^*. The large number of effector cells reduces the infected tumor cells to small numbers. However, since the available BCG (B^*) is also relatively small and does not increase with therapy b, infection of the tumor cells T_u is slowed down. As a result the high growth rate of the tumor cells T_u dominates and the tumor cannot be eradicated.

5. Discussion

We present here a new, relatively simple, mathematical model of BCG immunotherapy in superficial bladder cancer. The model exhibits multiple steady states, which depend on biologically related parameters and initial conditions. A clinically relevant feature of the model is the nontrivial dependence of the dynamics on the treatment rate b. Specifically, three distinct dynamical pattern can be distinguished, explicitly dependent upon the appropriate mode of tumor growth. The following dynamics occur (see Figs. 5–9):

1. For low treatment rates $b < r < p_2$, with growth term $\beta = 0$, an exponential expansion of the tumor is observed. For $\beta > 0$, there is logistic growth until the tumor-laden equilibrium is attained. Both of these correspond to clinical failure of BCG treatment.
2. For intermediate treatment rates $r/p_2 < b < \mu/p_2$ the tumor will be eradicated with only transient side effects. This results in the tumor-free equilibrium E_1^b. The tumor is eradicated exponentially fast as treatment intensity b increases (see (8)).
3. For high treatment rates $b > \mu/p_4$, the tumor mass will be eliminated, with permanent side effects that persist as long as BCG treatment is applied. This results in the so-called "side-effect" tumor-free equilibrium E_2^b which is characterized by an overdriven immune response.

In the case of logistic growth rate, bistability is often observed and any outcome will also depend on the initial conditions (as discussed below).

We will next discuss some possible limitations of the present study and the feasible future solutions to them. Finally, we will apply our results, to briefly discuss some possible causes for BCG treatment failure.

In our work, the complex biological processes of tumor, immune system, and BCG interactions are captured by a 4-dimensional system. Additional variables that would provide a more detailed description of the biology may obviously be envisioned. For example, Kirschner and Panetta (1998) have chosen to study the explicit effects of the immune cytokine interleukin-2 (IL-2) of the dynamics of the effector cells. In our model this effect is considered indirectly via the interaction terms such as $p_4 E B$ and αT_i. A more detailed characterization of the immune response may be explicitly considered by expansion of the model. Such is the case, for example, if we wish to analyze the possible favorable effect of augmenting BCG immunotherapy interferon-alpha2B (INF-α_{2B}) (Kassouf and Kamat, 2004).

A trade off between the analytical tractability and the reliability of the representation of the underlying biological system should always be taken into account. The need for additional complexity should ultimately be determined by experimental results that would either verify or contradict the model predictions. For example, the clinical fact that the spontaneous cure of TCC is very rarely observed (Papac, 1996) is accounted for in our model in that we do not allow for direct effect of the effectors cells on the uninfected tumor cells. Thus, with no or little treatment (low treatment rate $b < r/p_2$) the model will predict that no cure is possible. If on the other hand some immune response may be evoked even towards uninfected cells, this may change the dynamics. A clinical scenario in which additional antigenicity will be conveyed to the tumor by transgenic methods is currently being considered (Dumey et al., 2005). Such a trade off can also be invoked when concerning our approximation of BCG treatment at constant rate b. An analysis of a nonautonomous version of the model where pulses of treatment are explicitly accounted for is currently under way.

In this model, if continuous treatment is stopped and the (uninfected) cancer is not entirely removed from the bladder the tumor will always return to its untreated equilibrium. However, if there are no further uninfected cancer cells and treatment is stopped, the model will remain at the tumor-free equilibrium state, even though unstable. It will persist in this condition until the next cancer cell appears and the tumor will recur again. We speculate that the pulsed treatment scheme might offer a means to stabilize the tumor-free state.

The dynamical system studied here is space independent while the actual dynamics of tumor growth may have spatial dependency. For example, the actual bladder cancer initially spreads superficially upon the surface of the bladder, and is only several cells deep. This may indicate that the effect of the invasive properties and the nutrient-limited processes may need to be considered and studied, for example, with partial differential equations (such as in Franks et al., 2003). Moreover, as the invasion front is only on the periphery of the disk, the geometry of the tumor rim may affect the dynamics (see, for example, Bru et al., 2004). These considerations can be a scope for future models.

Finally, BCG is currently the most effective therapy in the prophylaxis of superficial TCC of the urinary bladder following primary resection (TUR). Yet, a significant fraction of patients fail the treatment (Nseyo and Lamm, 1997). In view that both the dose rate b and the tumor growth rate r are critical bifurcation parameters (Figs. 5, 6, 7, and 9), we wish to suggest that in many cases treatment failure stems from insufficient application of the dose rate b that does not match the appropriate value of r. The model predicts that there are cases where immunotherapy cannot help. In particular, Fig. 9b shows that high tumor growth rates can prevent immunotherapy from eradicating the tumor, no matter how strong the therapy might be. Noteworthy, our model suggests that if a feasible way of administrating continuous dose rate b can be devised, this will in many cases enable effective treatment. A specific suggestion about clinical feasibility of such an approach should be a theme of further studies and is beyond the scope of the current paper.

Moreover, due to the interesting feature of bistability, the outcome of BCG treatment is dependent on the initial conditions of tumor following surgical curettage. Thus, while some tumors may potentially respond to BCG treatment, the initial tumor burden may sit in the domain of attraction of the unfavorable steady state and ultimately result in treatment failure (Fig. 8). That initial conditions can further steer the treatment to either failure

or success may be the key to the observation that addition of intra-vesical chemotherapy prior to BCG treatment may be beneficial in some cases (Kaasinen et al., 2000).

Indeed an ultimate, but albeit still distant, application for the model is to aid in defining the appropriate rate of BCG instillation in a particular clinical situation. To enable such a potential application for individual bladder cancer patients, certain clinical parameters need to be measured prospectively:

- Repeated direct assessment of the tumor. The determination of the tumor area following TUR curettage will provide initial conditions for model input. Subsequent examinations will provide with the response to treatment. Though frequent observations by cystoscopy is hardly a feasible clinical option, alternative noninvasive monitoring of tumor status (for example, by radioactive imaging Chiou et al., 1999) could be considered.
- Calculation of the tumor properties. The growth rate can be obtained indirectly by assessment of bromodeoxyuridine (BrdU) incorporation or antigen Ki67 expression (Limas et al., 1993). Related features such the proliferation an invasive potential can be accessed by micro-array analysis (Modlich et al., 2004).
- Measurement of the actual BCG concentration in the bladder. Although the vast majority of the bacteria are cleared within several hours following instillation, some evidence exists that BCG persist in the bladder for much longer periods (Bowyer et al., 1995). This may alter the actual treatment rate b, which may be significant near the bifurcation points (see also the clinical implications section).
- Measurement of the rate of infection of the tumor cells with BCG and the rate of interaction of BCG with APC (see Durek et al., 1999 for elegant experiments).
- Measurement of the in vivo intra-bladder immune response. Here, the kinetics of urine cytokines may be considered as valuable surrogates (de Reijke et al., 1999).

Such dedicated experimental setting is beyond the ability of most practice oriented clinical institutions. However, given the prospect of potential cure in otherwise devastating disease, as may be hinted by our analysis, a search for an intense dialog with theoretically inclined clinicians is appropriate.

Acknowledgements

We thank Professors Helen Byrne and Leonid Polterovich, Dr Rob Bevers and Professor Sven Brandau for helpful comments and suggestions. We are grateful to David Bunimovich and Gal Zahavi for fruitful and stimulating discussions. This work was supported by the James S McDonnell Foundation.

Appendix A

Here we show that model equations (4) are Liapunov stable in the absence of BCG therapy ($b = 0$; Section 3.3.2). Recall that the positive orthant is invariant (see Section 3.1). The first equation in (4) with $b = 0$, implies that $\frac{dB}{dt} < 0$ for all t, and $B(t) \to 0$ as $t \to \infty$. As a consequence, the uninfected tumor growth follows the logistic model $\frac{dT_u}{dt} = rT_u(1 - \beta T_u)$

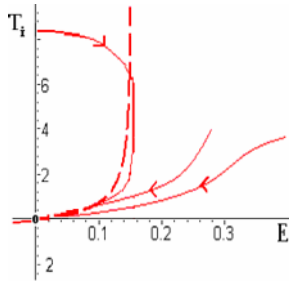

Fig. A.1 Different trajectories (solid lines) of model (A.1) as plotted in the phase plane. Effector cells (E) are plotted against infected tumor cells (T_i) for three different initial conditions. The dashed line portrays the E-nullcline (see the text above) where $\mathrm{d}E/\mathrm{d}t = 0$. The equilibrium at the origin is notated by o.

and thus $T_u \to T_u^* = 1/\beta$. Plugging $B = 0$ into (4), gives the following reduced system which approximates the model's dynamics:

$$\begin{aligned} \frac{\mathrm{d}E}{\mathrm{d}t} &= E(-\mu - p_5 T_i) + \alpha T_i, \\ \frac{\mathrm{d}T_i}{\mathrm{d}t} &= -p_3 E T_i. \end{aligned} \tag{A.1}$$

The Jacobian of this system about the equilibrium $(E^*, T_i^*) = (0, 0)$ is:

$$J = \begin{bmatrix} -\mu & \alpha \\ 0 & 0 \end{bmatrix}$$

and has eigenvalues $\overline{\lambda} = [-\mu, 0]$. Similar to (4), this simplified system retains a single zero eigenvalue whose influence may now be determined by phase plane analysis.

First note that $T_i = 0$ is an invariant line that cannot be crossed by the model's trajectory ensuring $T_i(t) \geq 0$ for all t, assuming a positive initial condition $T_i(0) > 0$. Also, it is clear that $\mathrm{d}E/\mathrm{d}t > 0$ when $E = 0$, and the trajectory is always repelled to the right away from the T_i-axis ($E = 0$) ensuring $E(t) > 0$ for positive initial conditions.

The E-nullcline is specified by the equation $\mathrm{d}E/\mathrm{d}t = 0$, namely: $T_i = \frac{\mu E}{\alpha - p_5 E}$. As seen in the phase plane diagram in Fig. A.1, trajectories above the E-nullcline in the positive orthant have $\mathrm{d}E/\mathrm{d}t > 0$, and those below have $\mathrm{d}E/\mathrm{d}t < 0$. Figure A.1 shows how trajectories are attracted to the equilibrium at the origin $E^* = T_u^* = 0$ by winding around the phase-plane. Thus according to the phase plane dynamics the system is stable despite the zero eigenvalue.

The stability of (A.1) may also be found through examining the Liapunov function:

$$V(E, T_i) = \frac{E^2}{2} + kT_i > 0,$$

where $k \geq 0$ arbitrary and the function $V(E, T_i)$ is positive definite on R_+^2 with $V(0, 0) = 0$. Examine now

$$\frac{\mathrm{d}V(E, T_i)}{\mathrm{d}t} = E\frac{\mathrm{d}E}{\mathrm{d}t} + k\frac{\mathrm{d}T_i}{\mathrm{d}t} = -\mu E^2 + \alpha E T_i - p_5 E^2 T_i - k p_3 E T_i.$$

If we choose: $k = \frac{\alpha}{p_3} > 0$ then:

$$\frac{\mathrm{d}V(E, T_i)}{\mathrm{d}t} = -\mu E^2 - p_5 E^2 T_i < 0.$$

Thus the Liapunov function V decreases with time and the trajectory of (A.1) must cross the level curves $V(E, T_i) = c$ as it is attracted to the origin $E^* = T_i^* = 0$. According to the Invariance Principle (Hale and Kocak, 1991, Theorem 9.22, p. 288), the equilibrium $E^* = T_i^* = 0$ is Liapunov stable and R_+^2 is a basin of attraction.

References

Alexandroff, A.B., Jackson, A.M., O'Donnell, M.A., James, K., 1999. BCG immunotherapy of bladder cancer: 20 years on. Lancet 353, 1689.

Andius, P., Holmang, S., 2004. Bacillus Calmette–Guérin therapy in stage Ta/T1 bladder cancer: prognostic factors for time to recurrence and progression. BJU Int. 93(7), 980–984.

Aranha, O., Wood, D.P., Sarkar, F.H., 2000. Ciprofloxacin mediated cell growth inhibition, S/G2-M cell cycle arrest, and apoptosis in a human transitional cell carcinoma of the bladder cell line. Clin. Cancer Res. 6, 891–900.

Archuleta, J., Mullens, P., Primm, T.P., 2002. The relationship of temperature to desiccation and starvation tolerance of the Mycobacterium avium complex. Arch. Microbiol. 178, 311–314.

Banks, R.B., 1994. Growth and Diffusion Phenomena. Springer, Berlin.

Bevers, R.F.M., Kurth, K.H., Schamhart, D.H.J., 2004. Role of urothelial cells in BCG immunotherapy for superficial bladder cancer. Br. J. Cancer 91, 607–612.

Bohle, A., Brandau, S., 2003. Immune mechanisms in bacillus Calmette–Guérin immunotherapy for superficial bladder cancer. J. Urol. 170, 964–969.

Bowyer, L., Hall, R.R., Reading, J., Marsh, M.M., 1995. The persistence of bacille Calmette–Guérin in the bladder after intravesical treatment for bladder cancer. Br. J. Urol. 75(2), 188–192.

Bru, A., Albertos, S., Garcia-Asenjo, J.A.L., Bru, I., 2004. Pinning of tumoral growth by enhancement of the immune response. Phys. Rev. Lett. 11 92(23), 238101.

Chen, F., Zhang, G., Iwamoto, Y., See, W., 2005. BCG directly induces cell cycle arrest in human transitional carcinoma cell lines as a consequence of integrin cross-linking. BMC Urol. 5, 8.

Cheng, C.W., Ng, M.T., Chan, S.Y., Sun, W.H., 2004. Low dose BCG as adjuvant therapy for superficial bladder cancer and literature review. ANZ J. Surg. 74(7), 569–572.

Chiou, R.K., Dalrymple, G.V., Baranowska-Kortylewicz, J., Holdeman, K.P., Schneiderman, M.H., Harrison, K.A., Taylor, R.J., 1999. Tumor localization and systemic absorption of intravesical instillation of radio-iodinated iododeoxyuridine in patients with bladder cancer. J. Urol. 162(1), 58–62.

Chopin, D., Gattegno, B., 2002. Superficial bladder tumors. Eur. Urol. 42, 533–541.

De Boer, E.C., Bevers, R.F., Kurth, K.H., Schamhart, D.H., 1996. Double fluorescent flow cytometric assessment of bacterial internalization and binding by epithelial cells. Cytometry 25, 381–387.

De Pillis, L.G., Radunskaya, A.E., Wiseman, C.L., 2005. A validated mathematical model of cell-mediated immune response to tumor growth. Cancer Res. 65(17), 7950–7958.

De Pillis, L.G., Gu, W., Radunskaya, A.E., 2006. Mixed immunotherapy and chemotherapy of tumors: modeling, applications and biological interpretations. J. Theor. Biol. 238, 841–862.

De Reijke, T.M., De Boer, E.C., Kurth, K.H., Schamhart, D.H., 1999. Urinary interleukin-2 monitoring during prolonged bacillus Calmette-Guerin treatment: can it predict the optimal number of instillations? J. Urol. 161(1), 67–71.

Dumey, N., Mongiat-Artus, P., Devauchelle, P., Lesourd, A., Cotard, J.P., Le Duc, A., Marty, M., Cussenot, O., Cohen-Haguenauer, O., 2005. In vivo retroviral mediated gene transfer into bladder urothelium results in preferential transduction of tumoral cells. Eur. Urol. 47(2), 257–263.

Durek, C., Brandau, S., Ulmer, A.J., Flad, H.D., Jocham, D., Bohle, A., 1999. Bacillus Calmette–Guerin (BCG) and 3D tumors: an in vitro model for the study of adhesion and invasion. J. Urol. 162, 600–605.

Elkabani, M., Greene, J.N., Vincent, A.L., VanHook, S., Sandin, R.L., 2000. Disseminated Mycobacterium bovis after intravesicular bacillus Calmette–Guérin treatments for bladder cancer. Cancer Control 7(5), 476–481.

Franks, S.J., Byrne, H.M., King, J.R., Underwood, J.C., Lewis, C.E., 2003. Modelling the early growth of ductal carcinoma in situ of the breast. J. Math. Biol. 47(5), 424–452.

Hale, J.K., Kocak, H., 1991. Dynamics and Bifurcations. Springer, Berlin.

Kaasinen, E., Rintala, E., Pere, A.K., Kallio, J., Puolakka, V.M., Liukkonen, T., Tuhkanen, K., 2000. Weekly mitomycin C followed by monthly bacillus Calmette–Guérin or alternating monthly interferon-alpha2B and bacillus Calmette–Guérin for prophylaxis of recurrent papillary superficial bladder carcinoma. J. Urol. 164(1):47–52.

Kassouf, W., Kamat, A.M., 2004. Current state of immunotherapy for bladder cancer. Expert. Rev. Anticancer Ther. 4(6), 1037–1046.

Kim, J.C., Steinberg, G.D., 2001. The limits of bacillus Calmette-Guerin for carcinoma in situ of the bladder. J. Urol. 165(3), 745–756.

Kirschner, D., Panetta, J., 1998. Modelling immunotherapy of the tumor-immune interaction. J. Math. Biol. 37(3), 235–252.

Kuznetsov, V.A., Makalkin, I.A., Taylor, M.A., Perelson, A.S., 1994. Nonlinear dynamics of immunogenic tumours: parameter estimation and global bifurcation analysis. Bull. Math. Biol. 56, 295–321.

Lamm, D.L., Mcgee, W.R., Hale, K., 2005. Bladder cancer: current optimal intravesical treatment. Urol. Nurs. 25(5), 323–332.

Lakshmikantham, V., Bainov, D.D., Simeonov, P.S., 1989. Theory of Impulsive Differential Equations. World Scientific, Singapore.

Lämmle, M., Beer, A., Settles, M., Hanning, C., Schwaibold, H., Drews, C., 2002. Reliability of MR imaging-based virtual cystoscopy in the diagnosis of cancer of the urinary bladder. Am. J. Roentgenol. 178, 1483–1488.

Limas, C., Bigle, A., Bair, R., Bernhart, P., Reddy, P., 1993. Proliferative activity of urothelial neoplasms: comparison of BrdU incorporation, Ki67 expression, and nucleolar organiser regions. J. Clin. Pathol. 46(2), 159–165.

Modlich, O., Prisack, H.B., Pitschke, G., Ramp, U., Ackermann, R., Bojar, H., 2004. Identifying superficial, muscle-invasive, and metastasizing transitional cell carcinoma of the bladder: use of cDNA array analysis of gene expression profiles. Clin. Cancer Res. 10(10), 3410–3421.

Morales, A., Eidinger, D., Bruce, A.W., 1976. Intracavitary bacillus Calmette–Guérin in the treatment of superficial bladder tumors. J. Urol. 116, 180.

Nseyo, U.O., Lamm, D.L., 1997. Immunotherapy of bladder cancer. Semin. Surg. Oncol. 13, 342–349.

Papac, R.J., 1996. Spontaneous regression of cancer. Cancer Treat. Rev. 22(6), 395–423.

Patard, J.J., Saint, F., Velotti, F., Abbou, C.C., Chopin, D.K., 1998. Immune response following intravesical bacillus Calmette–Guérin instillations in superficial bladder cancer: a review. Urol. Res. 26(3), 155–159.

Press, W., Teukolsky, T., Vetterling, W.T., Flannery, B.P., 1992. Numerical Recipes. Cambridge University Press, New York.

Schenk-Braat, E.A.M., Bangma, C.H., 2005. Immunotherapy for superficial bladder cancer. Cancer Immunol. Immunother. 54(5), 414–423.

Shochat, E., Hart, D., Agur, Z., 1999. Using computer simulations for evaluating the efficacy of breast cancer chemotherapy protocols. Math. Models Meth. Appl. Sci. 9(4), 599–615.

Spratt, J.A., Von Fournier, D., Spratt, J.S., Weber, E.E., 1993. Decelerating growth and human breast cancer. Cancer 71(6), 2013–2019.

Swanson, K.R., Bridge, C., Murray, J.D., Alvord, E.C., 2003. Virtual and real brain tumors:using mathematical modeling to quantify glioma growth and invasion. J. Neurol. Sci. 216, 1–10.

Wigginton, J., Kirschner, D., 2001. A model to predict cell-mediated immune regulatory mechanisms during human infection with mycobacterium tuberculosis. J. Immunol. 166, 1951–1967.